



Research Paper

***Perilla frutescens* sprout extract protect renal mesangial cell dysfunction against high glucose by modulating AMPK and NADPH oxidase signaling**

Accepted

ABSTRACT

Perilla frutescens (L.) Britt. var. japonica (Hassk.) Hara (PF), is a medical herb of the Lamiaceae family. We previously reported the antidiabetic effect of PF sprout extract (PFSE). However, the role of PFSE on glomerular mesangial cells (MCs) proliferation and extracellular matrix (ECM) accumulation in diabetic condition is still unclear. Therefore, in this study, we investigated the role of PFSE on cell proliferation and ECM accumulation in murine glomerular MCs (MMCs) cultured under high glucose (HG) condition. PFSE treatment attenuated HG-induced MMCs proliferation and hypertrophy. Moreover, HG-induced ECM protein, collagen IV and fibronectin; overexpression was abolished by PFSE treatment. Also, PFSE inhibited ROS overproduction and NOX2 and NOX4 expression in MMCs under HG condition. Our data further showed the involvement of mesangial cells damage in AMPK activation. PFSE strongly activated AMPK in MMCs under hyperglycemic conditions. These results suggest that PFSE inhibits HG-mediated MC fibrosis through suppressing the activation of NOX2/4 and AMPK activation mechanism. PFSE may be useful for the prevention or treatment of diabetic nephropathy.

Ha-Rim Kim and Seon-Young Kim*

JeonjuAgroBio-Materials Institute,
54810, Wonjangdong-gil 111-27,
Deokjin-gu, Jeonju-si, Jeollabuk-do,
Republic of Korea.

*Corresponding author. E-mail:
Seon02@jbmi.re.kr. Tel: 82-63-711-
1053. Fax: 82-63-711-1004.

Key words: *Perilla frutescens*, murine mesangial cells, diabetic nephropathy, reactive oxygen species (ROS), NADPH oxidase.

INTRODUCTION

Diabetic nephropathy (DN) is a leading cause of end-stage renal disease and is associated with increased mortality and morbidity (Ritz et al., 1999). DN is characterized by the progressive expansion of the mesangium with accumulation of extracellular matrix (ECM) in the glomerulus (Mason and Wahab, 2003). Glomerular mesangial cells (MCs) proliferation, hypertrophy, and ECM accumulation are hallmarks of diabetic nephropathy (Ziyadeh 1993, Mason and Wahab, 2003).

Reactive oxygen species (ROS) are ubiquitous, highly reactive short-lived derivatives of oxygen metabolism produced in all biological systems that react with surrounding molecules at the site of formation. It has been known that ROS, at a low level, play an essential role in multiple cellular signal transduction pathways. However, under conditions of oxidative stress, they contribute to a

series of cellular dysfunctions. Several studies support the finding that renal ROS play a central role in mediating renal injury in diabetes (Gill and Wilcox, 2006; Calcutt et al., 2009; Gorin and Block, 2013). It has been reported that ROS play an important role in the pathogenesis of renal profibrotic factors in inducing fibroblast proliferation and/or activation (Manickam et al., 2014). Our previous studies also confirmed that the ROS were increased in MCs under high-glucose conditions (Jeong et al., 2012). NADPH oxidases (NOX) are important sources of ROS involvement in both normal physiological functions and oxidative stress (Gill and Wilcox, 2006).

AMP-activated kinase (AMPK) is a cellular energy sensor that exerts diverse biological effects on cell growth, differentiation, and apoptosis, as well as the regulation of glucose and lipid metabolism. AMPK activators mimic the

actions of insulin in terms of gluconeogenesis, repressing glucose production (Hardie et al., 2012; Carling, 2017). Reduced expression and/or inhibition of AMPK activity has been involved in pathogenesis of DN (Kim et al., 2013). Numerous cellular and animal experiments report cardiovascular-protective effects of AMPK. Several lines of research indicate that AMPK activation may function as a NOX inhibition (Song and Zou, 2012).

Perilla frutescens (L.) Britt. var. japonica (Hassk.) Hara (PF), commonly called perilla or Korean perilla, is a species of perilla belonging to the mint family Lamiaceae. It is a well-known annual herbaceous plant, often used in foods and medicine in Asia countries such as Korea, China, and Japan. This plant is commonly known as “Dlggae” in Korea (Kim et al., 2018). Previously, we reported antioxidant and hypoglycemic effects of PF sprout extract (PFSE) in pancreatic β -cells and type 2 diabetic animal model (Hye et al., 2017; Kim et al., 2018). However, the protective effect of PFSE against DN and the underlying mechanism remains elusive. Based on this background, the present study investigated the effect of PFSE on DN in murine MCs.

MATERIALS AND METHODS

Chemicals and antibodies

Phosphate-buffered saline (PBS), Dulbecco's modified Eagle's medium (DMEM), fetal bovine serum (FBS), and antibiotics (amphotericin B, penicillin, and streptomycin) were purchased from Invitrogen (Carlsbad, CA, USA). Dimethyl sulfoxide (DMSO), 2',7'-dichlorofluorescein diacetate (DCF-DA), diphenylene iodonium (DPI), and other chemicals were obtained from Sigma (St Louis, Mo, USA). Antibodies were obtained as follows: anti-phospho-AMPK pAb, anti-AMPK pAb, and anti-NOX4 pAb, anti-NOX2 (gp91phox)pAb, and anti-fibronectin pAb, and horseradishperoxidase(HRP)-conjugated anti-mouse IgG, anti-goat IgG, and anti-rabbit IgG were purchased from Santa Cruz Biotechnology (SantaCruz, CA).

Preparation of samples for treatment

PF sprouts were obtained from Aeong association (Jinan, Jeonbuk, Korea) and the extract was prepared using the standard procedure described previously (Kim et al., 2018). In summary, dried sprouts were extracted in 40% aqueous ethanol (EtOH) for 5 h at 70°C. After filtering the extracts, the solvents were rotary-vacuum evaporated and then freeze dried. The extraction yield from dry weight of PF sprouts was 15%.

Culture of MMCs

SV40-transformed MMCs (MES-13) were obtained from

America Type Culture Collection (ATCC; Rockville, MD, USA) and maintained in DMEM containing 5% FBS, 0.25 μ g/ml amphotericin B, 100 units/ml penicillin, and 100 units/ml streptomycin at 37°C in 5% CO₂, 95% air. Cells were passaged three times per week.

Proliferation assay

Cells were seeded at a density of 5×10^3 cells/well in a 96-well plate. When the cells reached 60-70% confluence, the growth medium was aspirated and the wells were rinsed with pre-warmed PBS. Quiescent cells were exposed to a fresh medium with different concentrations of PFSE (0.1 ~ 100 μ M) or 0.1% DMSO (vehicle control) for 48 h. After incubation, 20 μ L of a solution of Cell Titer 96 Aqueous One Solution (Promega, Madison, WI, USA) containing MTS [3-(4,5-dimethylthiazol-2-yl)-5-(3-carboxymethoxyphenyl)-2-(4-sulfophenyl)-2H-tetrazolium] and an electron coupling reagent (phenazine ethosulfate) were added to each well. The plates were incubated for 3 h during which time the reagent was bio-reduced into a colored formazan product by the intracellular dehydrogenase enzymes of metabolically active cells. The absorbance was measured at 490 nm (Perkin Elmer, Victor² 1420 Multilabel counter).

Determination of DNA synthesis

A total of 1×10^4 MMCs/well were seeded onto 96-well plates and grown to semiconfluence in DMEM containing a normal glucose concentration and 5% FBS for 24 h. The cells were washed once with PBS before growth arresting in DMEM without FBS for 48 h. Quiescent MCs were stimulated with HG and pretreated with different concentrations of PFSE (0.1 ~ 100 μ g/mL) for 48 h. DNA synthesis was quantified by 5-bromo-2'-deoxyuridine (BrdU) incorporation into proliferating cells for over 2 h (Roche Diagnostics, Mannheim, Germany).

Total protein to cell count ratio

The ratio of total protein content to cell number is another well-established measurement of cellular hypertrophy (Wolf et al., 2001). To measure this ratio, MMCs were seeded into each well of a six-well plate and were synchronized into quiescence for 12 h in serum free medium containing a normal glucose concentration. MCs were stimulated with HG and pretreated with different concentrations of PFSE (10 ~ 100 μ g/ml) for 48 h. After incubation, cells were trypsinized, scraped off the plate with a rubber policeman, and washed twice in PBS. A small aliquot of cells was used for cell counting of intact viable cells after trypan blue (Biochrom, Germany) staining to calculate the cell number/protein ratio. The remaining cells were lysed in RIPA buffer (10 mM Tris/HCl (pH 7.4), 150

mM NaCl, 10 mM EGTA, 10 mM EDTA, 10 mM sodium pyrophosphate, 1 mM sodium orthovanadate, 50 mM sodium fluoride, 1% (v/v) Triton X-100, 20 μ M leupeptin, 1 mM PMSF and 0.15 μ M pepstatin, and total protein content was measured using the Bradford method. Total protein content was expressed as μ g protein per 10^4 cells. These experiments were independently carried out three times.

Measurement of ROS

Generation of intracellular ROS was measured with the fluorophore DCF-DA. Briefly, MMCs were incubated for 60 min at 37°C with 10 μ M DCFDA in absence or presence of PFSE in a dose-dependent manner. Fluorescence intensity was measured by fluorescence microscopy (NIKON; excitation 488 nm, emission 513 nm). Average intensity for each experimental group of cells was determined using Scion Image Analysis software, and values were expressed as above control.

Determination of superoxide anion production activity

Superoxide anion production by mesangial cells was determined by measuring the superoxide dismutase-inhibitable reduction of cytochrome c with a spectrophotometer as previously described (Chen et al., 1997). Briefly, the mesangial cells were grown in 24-well tissue culture plates. The cells were treated with various inhibitors, containing cytochrome c (80 μ M) with or without superoxide dismutase (100 μ g/ml). The absorbance was then measured with a spectrophotometer at 550 nm. The relative amount of superoxide anions secreted by cells was calculated.

Determination of reduced glutathione levels in MMCs

Reduced glutathione (GSH) content was determined in mesangial cells lysates. GSH content was carried using glutathione assay kit (Cayman, MI, USA). The kit is based on an enzymatic recycling method, using glutathione reductase for the quantification of GSH.

Immunoblotting

Protein extraction and immunoblotting of MMCs were performed as previously described (Kim et al., 2008). Proteins (20 μ g per lane) were resolved on a 10% or 12% SDS-PAGE gel and transferred to polyvinylidene difluoride (PVDF, GE Healthcare, Little Chalfont, Buckinghamshire, UK) membranes. Blots were incubated with primary antibodies (1:2,500 dilution of each antibody) overnight at 4°C. The blots were rinsed four times with blocking buffer and

incubated with horseradish peroxidase-conjugated secondary antibodies (1:5,000 dilutions of each antibody) for 1 h at room temperature. The binding of the antibodies was visualized using an enhanced chemiluminescence (ECL) system (Bio-Rad, Munich, Germany). Protein concentrations were determined using a Bio-Rad protein assay kit and known concentrations of bovine serum albumin (BSA) were used as the standard. All immunoreactive signals were analyzed by densitometric scanning (Fuji Photo Film Co., Tokyo, Japan).

Statistical analysis

Data were represented as means \pm standard deviation (SD) of at least three separate experiments. Statistical comparisons were performed using one-way ANOVA followed by the Scheffé's test. Statistical significance of difference between groups was determined using the Student's t test. Differences were considered significant if the P value was less than 0.05.

RESULTS

Effects of PFSE on high glucose (HG)-induced MMCs growth and hypertrophy

Since one of the earliest renal abnormalities observed after the onset of hyperglycemia commonly includes the proliferation of MCs, PFSE was tested for ability to inhibit MMCs proliferation under HG (25 mmol/L) condition. HG-stimulated proliferation was evaluated using MTS and BrdU incorporation assay. HG stimulated the growth of MMCs as compared with NG (5.5 mmol/L) condition ($P < 0.01$). Diphenylene iodonium (DPI), a NADPH oxidase (NOX) inhibitor, and metformin (Met), an AMPK activator, both significantly inhibited HG induced-proliferation of MMCs (Figure 1A and B) as analyzed by MTS and BrdU incorporation. PFSE pretreatment with different concentrations (0.1 ~ 100 μ g/mL) showed significant inhibition of cell growth stimulated by HG (Figure 1A and B), the threshold concentration of PFSE that caused inhibition of proliferation was 50 μ g/mL ($130.7 \pm 21.2\%$ vs $173.2 \pm 21.8\%$, $P < 0.05$), with maximal effect at 100 μ g/mL ($113.9 \pm 7.8\%$ vs $173.2 \pm 21.8\%$, $P < 0.001$) as showed in MTS assay (Figure 1A). Similar results were obtained using BrdU incorporation assay (Figure 1B). Unlike HG, the addition of 25 mM mannitol (HM) to the media did not affect the proliferation of MMCs as compared with the control, suggesting that the HG-triggered mesangial cell growth is not the result of high osmolality within the media. The morphological change in DN is mesangial cell hypertrophy, which results from an increase in protein synthesis in the early phase of hyperglycemia. As shown in Figure 1C and D, cell morphology and the ratio of the

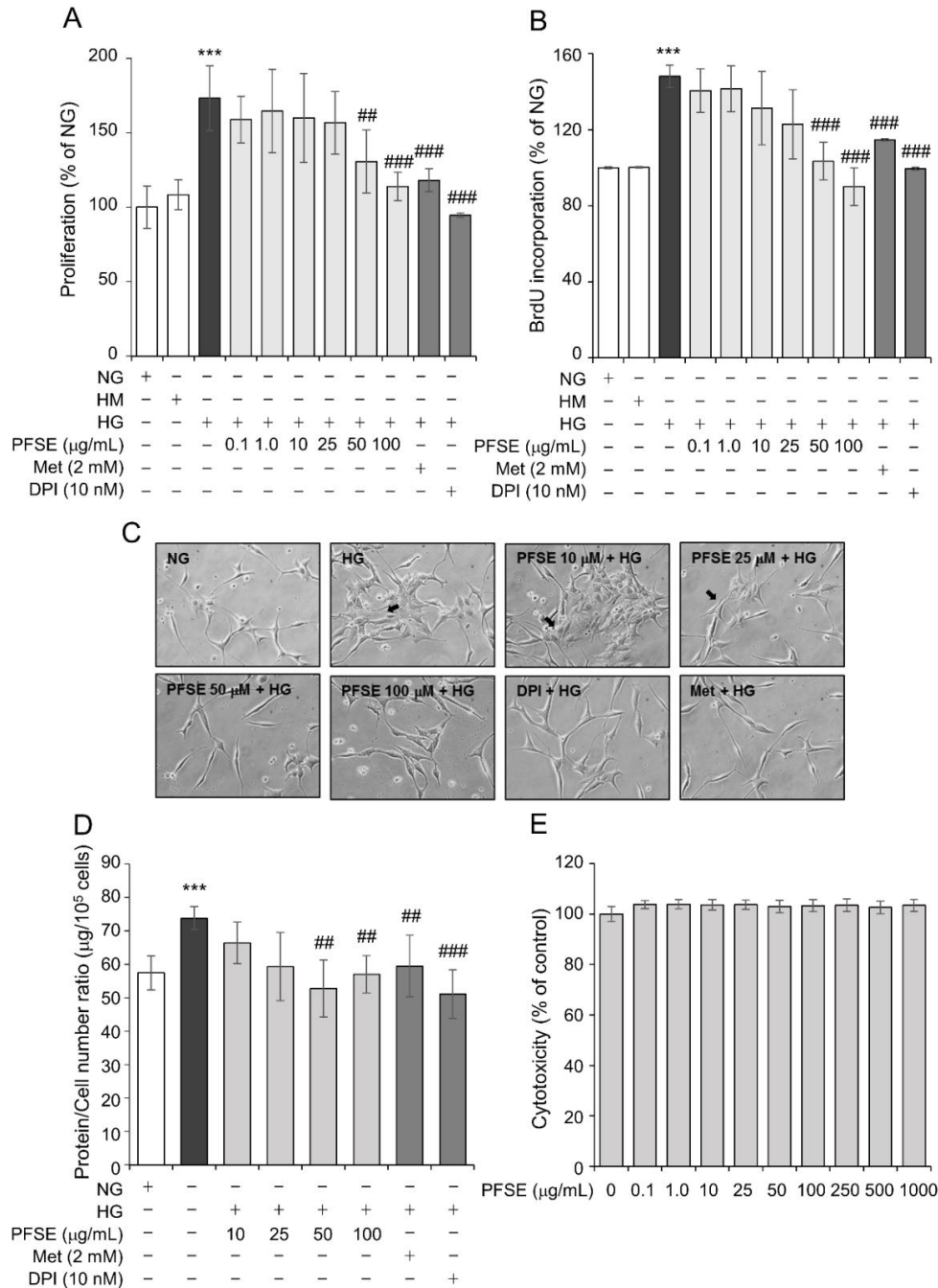


Figure 1: Effect of *Perilla frutescens* sprout extract (PFSE) on high glucose (HG)-induced proliferation and protein synthesis in murine mesangial cells (MMCs). (A) MMCs were treated with HG (25 mM) for 48 h in the absence or presence of PFSE (0.1, 1.0, 10, 25, 50 and 100 µg/mL), Met (metformin, 2 mM), and DPI (diphenylene indonium, 10 nM). After this incubation, cell proliferation was determined with the MTS assay. (B) PFSE inhibits HG-induced DNA synthesis in MMCs. DNA synthesis was measured using BrdU cell proliferation assay. (C) Representative microscopic images of cells under normal glucose (NG, 5.5 mM) or HG conditions in a presence or absence PFSE, Met, and DPI. (D) The total protein/cell number ratio expressed as µg/10⁵ cells after PFSE treatment for 48 h. (E) Cellular cytotoxicity of PFSE in HEK-293T cells. ****P* < 0.001 vs. normal glucose (NG, 5.5 mM); ##*P* < 0.01, ###*P* < 0.001 vs. HG. Values are means ± SEM of three independent experiments.

amount of total protein to cell number in MMCs under HG condition were significantly greater than NG group (*P* <

0.001). PFSE treatment abolished the MMCs hypertrophy from 50 µg/mL. The NOX inhibitor and AMPK activator also

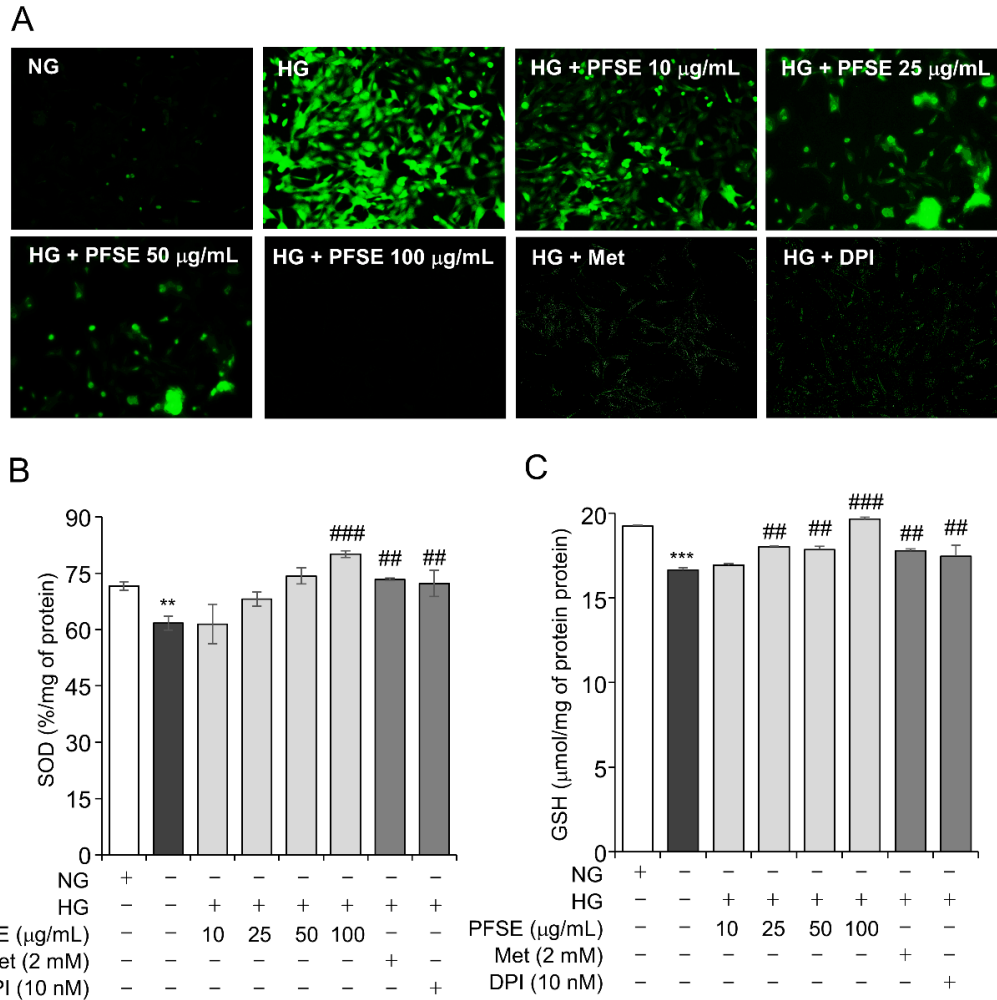


Figure 2: PFSE inhibits HG-induced oxidative stress in MMCs. (A) MMCs were treated with HG in the presence or absence of PFSE (10, 25, 50 and 100 μ g/mL), Met (2 mM), and DPI (10 nM) for 48 h. Cells were stained with ROS-sensitive dye 2',7'-dichlorofluorescein diacetate (DCFDA) and observed under a fluorescence microscope. (B) The effects of PFSE on antioxidant enzyme, superoxide dismutase (SOD) activity. (C) Intracellular reduced glutathione (GSH) in mesangial cells, cultured in 5.5 or 25 mM glucose with or without PFSE, Met, and DPI for 48 h. ** P < 0.05 vs. NG, ### P < 0.01, #### P < 0.001 vs. HG. Values are means \pm SEM of three independent experiments.

remarkably blocked protein synthesis of MMCs. These data suggest that HG-induced proliferation and hypertrophy is mediated by NOXs and AMPK signaling. In addition, PFSE treatment did not have effect on cell growth in MMCs as compared with the control at the tested concentration (0.1 ~ 1,000 μ g/mL), which explains an inhibitory effect of PFSE on proliferation and hypertrophy rather than the cytotoxic effect (Figure 1E).

PFSE reduces reactive oxygen species (ROS) production and increases the activity of antioxidant enzymes

Due to the crucial role of ROS in renal damage and the property of HG, we tested the antioxidative effect of PFSE by HG in MMCs. In our previous results (Kim et al., 2018), PFSE have an antioxidant effect in pancreatic β -cells. As shown in

Figure 2A, HG stimulated intracellular ROS increase in MMCs. PFSE treatment notably decreased the ROS in a dose-dependent manner. HG significantly decreased the activity of SOD and GSH (P < 0.01 and P < 0.001, respectively), as shown in Figure 2B and C. Treatment of PFSE increased the SOD activity and GSH levels in cells. In addition, DPI and Met also significantly inhibited the intracellular ROS increase and stimulates antioxidant enzymes (Figure 2B). These data suggest that PFSE has significant antioxidative effects against HG-induced oxidative stress in MMCs.

PFSE regulates HG-induced NOX and AMPK activation

We next evaluated the molecular mechanisms which are responsible for the protective effects of PFSE. Since NOX

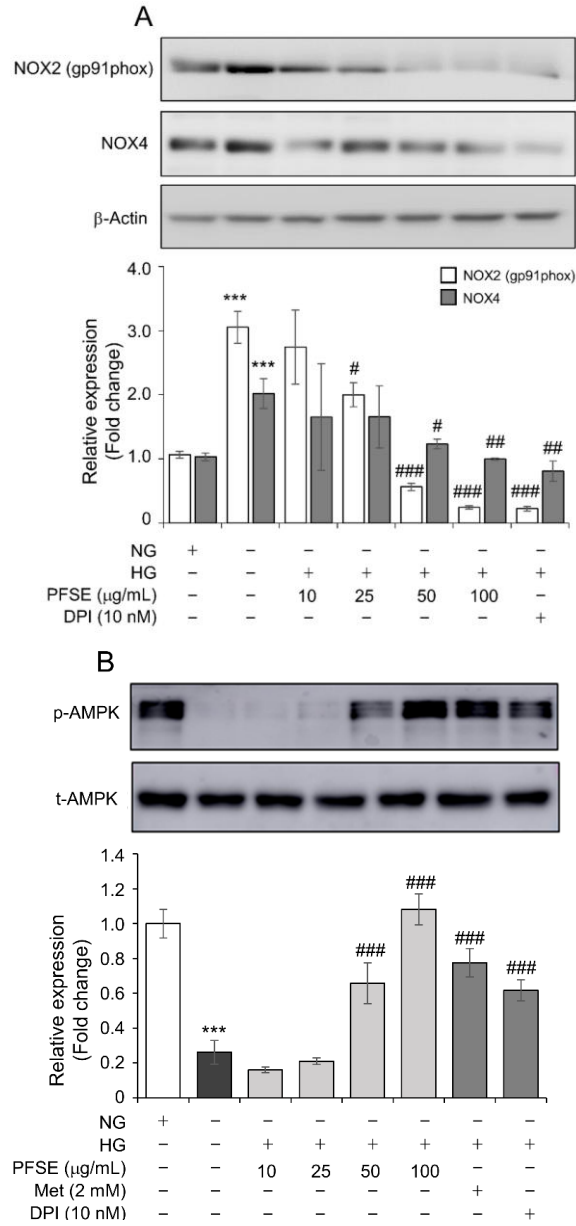


Figure 3: HG-mediated NADPH oxidase (NOX) overexpression and AMPK dephosphorylation was inhibited by PFSE. (A) The protein levels of NOX2 and NOX4 after 48 h of HG treatment were determined by immunoblotting. PFSE (10, 25, 50, and 100 μ M) pretreatment blocked HG-induced NOX protein overexpression. Relative expression of each protein corresponding to β -actin was presented in lower panel. (B) The effect of varying concentration of PFSE on AMPK phosphorylation was assessed by western blot. Densitometric data of p-AMPK relative to t-AMPK are presented in lower panel. *** P < 0.001 vs. NG; # P < 0.05, ## P < 0.01, ### P < 0.001 vs. HG. Values are means \pm SEM of three independent experiments.

family have been demonstrated to produce the majority of intracellular ROS increase in renal injury (Gill and Wilcox, 2006; Jeong et al., 2012), we investigated the effects of PFSE on NOXs activation in MMCs. The expression of NOX2

(gp91phox) and NOX4, a major source for ROS in the kidneys, was significantly up-regulated in MMCs under HG conditions, and this was ameliorated by PFSE in a dose dependent manner (Figure 3A). As shown in Figure 1,

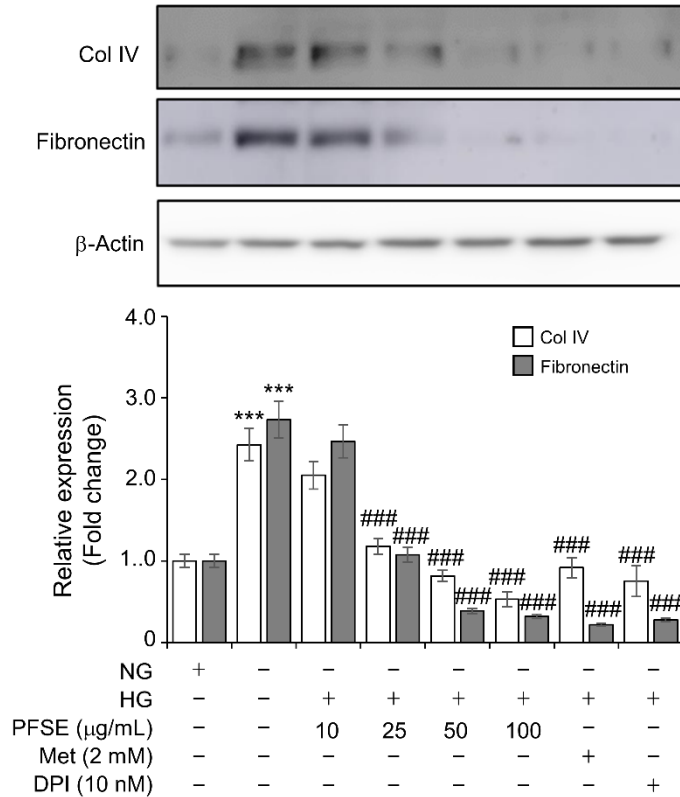


Figure 4: Sch pretreatment causes a decrease in extracellular matrix (ECM) protein accumulation in MMCs under HG condition. Comparison of expression of Col IV (type IV collagen) and fibronectin in MMCs. Relative expression of each protein compared with β -actin. *** $P < 0.001$ vs. NG; ### $P < 0.001$ vs. HG. Values are means \pm SEM of three independent experiments.

pretreatment with Met (2 mM) dramatically blocked the proliferation and hypertrophy of MMCs under HG conditions. To evaluate the role of PFSE with respect to AMPK activation, PFSE was treated to cells under HG conditions in MMCs. The levels of pAMPK decreased markedly in MMCs under HG condition, and this was reversed by pretreatment of MMCs with PFSE from 50 μ g/mL concentration. Met and DPI also reserved HG-induced AMPK phosphorylation (Figure 3B). These results suggest that PFSE blocked HG-induced proliferation and protein synthesis of mesangial cells via NOX-induced ROS increase inhibition, as well as AMPK activation.

PFSE reversed the effect of HG on expression of extracellular matrix (ECM) protein

The efficacy of PFSE on HG-induced fibrosis was evaluated by determining the protein expression of kidney fibrosis-related proteins. Increased synthesis of ECM proteins, such as type IV collagen (Col IV) and fibronectin, are regarded as the makers of proliferative nephritis (Floege et al., 1991; Ziyadeh, 1993). HG significantly increased the protein

expression of Col IV and fibronectin in MMCs ($P < 0.001$), which was remarkably abrogated by PFSE pretreatment with 25 ~ 100 μ g/mL ($P < 0.001$) (Figure 4). The findings presented here demonstrated that PFSE could also inhibit HG-induced ECM production in MMCs.

DISCUSSION

Our previous studies have suggested that PFSE have the potential to protect against the development of diabetes via modulation of the AMPK pathway (Kim, Kim et al. 2018). The effective concentration was higher than 100 μ g/mL in HepG2 cells. DN is the major cause of chronic renal failure in diabetes mellitus (DM) (Ritz et al., 1999; Dronavalli et al., 2008). Previously, we also reported that RA was the major compound in PF sprout (Kim et al., 2018). Studies reported that RA exerts renal protective role to DN and has antioxidant and anti-inflammatory activity (Petersen and Simmonds 2003; Erkan et al., 2008; Jiang et al., 2012). However, whether PF sprout can attenuate renal damage has not been determined. In this study, we demonstrated that PFSE is potent in reducing high glucose-mediated

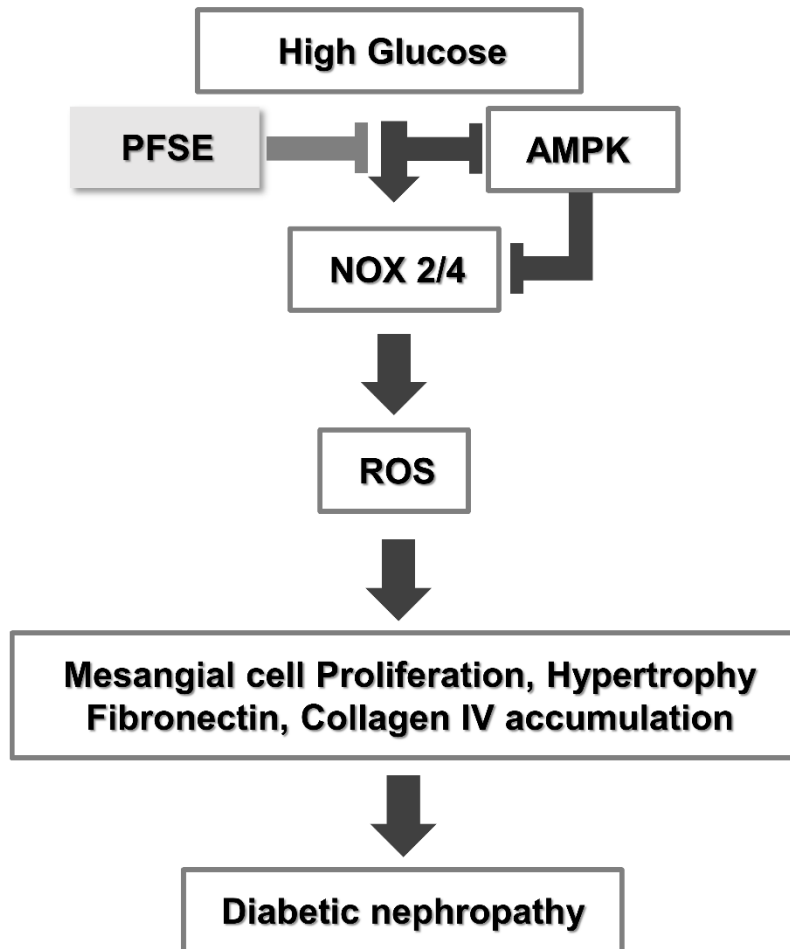


Figure 5: PFSE protects HG-mediated mesangial cell damage via NADPH oxidase and AMPK signaling regulation. High glucose stimulates NADPH oxidases activation and reduces AMPK activity in mesangial cells. Upon activation, NADPH oxidase leading to ROS increase, endogenous antioxidant's reduction, and stimulate mesangial cell damage. PFSE may protect against HG-induced proliferation, hypertrophy, and ECM protein accumulation by inhibiting this pathway.

murine mesangial cells proliferation and fibrosis, by regulating AMPK and NOX-derived ROS generation with an effective concentration of 25 ~ 100 $\mu\text{g}/\text{mL}$ (Figure 5).

DM is associated with an increase in the generation of ROS, in the kidney, which is involved in glomerulosclerosis. NOX is the major sources of ROS in renal cells. NOX catalyzes the production of O_2^- by the non-electron reduction of O_2 using NAD(P)H as the electron donor. NOX hyperactivation leads to excessive ROS generation that disrupts redox network, normally regulated by antioxidant systems, resulting in oxidative stress, which triggers molecular processes contributing to tissue injury. Several NOX families have been identified, including NOX1-7, of which NOX1, 2, and 4 activity are altered by diabetes, or diabetic complication. The most extensively studied NOX isoform is the phagocyte NOX2 (gp91phox), which requires regulatory subunits such as the small transmembrane protein p22phox, and the cytosolic regulatory subunits

p47phox and p67phox (Nauseef, 2004). Unlike all the other NOX proteins, NOX4 is constitutively active and is independent of cytosolic activator proteins or regulatory domains. Among the NOX families, NOX2 and NOX4 have been identified to be involved in HG-dependent oxidative stress and fibronectin or Col IV accumulation in MCs (Xia et al., 2006; Zhang et al., 2012). SOD is the major antioxidant enzyme, and it converts superoxide into hydrogen peroxide and molecular oxygen (Fridovich 1997). GSH, a well-known defensive antioxidant and a cofactor of glutathione peroxidases, is capable of preventing ROS-induced cellular damage (Pompella et al., 2003). In our study, PFSE treatment inhibited HG-induced ROS generation, as well as prevent SOD inactivation and GSH reduction in MMCs (Figure 2). The NOX2 and NOX4 overexpression was also attenuated by PFSE treatment under hyperglycemic conditions in MMCs (Figure 3A).

AMPK is a ubiquitously expressed heterotrimeric kinase,

which is a regulator of cellular energy homeostasis. It consists of an α , β , and a γ subunit and is activated via phosphorylation of threonine residue 172 (Hardie et al., 2012, Kume et al., 2012). It is expressed in the kidney, where it is involved in diverse physiological and pathologic processes, including ion transport, podocyte function, and diabetic renal hypertrophy (Kim and Park, 2016). In addition, a recent study showed that AMPK phosphorylation was also reduced by nearly 70% in renal cortex of *db/db* mice, a model of T2DM (Lee et al., 2007). AMPK has also been closely linked to fibrosis promoting pathways. Several groups have reported that AMPK activation was able to reduce mesangial matrix expansion and urinary TGF- β 1 levels, as well as inhibit glomerular collagen and fibronectin accumulation in mouse models of diabetic kidney disease (Dugan et al., 2013; Declèves et al., 2014; Sharma, 2014).

It was reported that AMPK activation have a potent ability to reduce NOX activation and H₂O₂ production (Song and Zou, 2012; Sharma, 2014; Kumar, 2016). Whereas, Banskota et al. (2015) reported that AMPK phosphorylation was suppressed by NOX2-activated ROS production in an invasive phenotype response in human colon cancer cells (HT29) (Banskota et al., 2015). In addition, it has been reported that ROS can directly regulate AMPK activity (Hinchy et al., 2018). Consistent with prior reports, AMPK activator also inhibited HG-induced oxidative stress in MMCs (Figure 2). Our results also showed that NOX inhibitor blocked AMPK inactivation in MMCs under hyperglycemic conditions (Figure 3B). It was also shown that PFSE prevented HG-stimulated AMPK dephosphorylation in MMCs. Finally, PFSE attenuated HG-induced ECM accumulation via downregulation of Col IV and fibronectin protein in mesangial cells (Figure 4).

In conclusion, the present study provides evidence that PFSE attenuated proliferation and hypertrophy, ROS generation, and inactivation of SOD and reduction of GSH levels in MMCs under hyperglycemic conditions, which may contribute to its renoprotective effects of DN. Interestingly, PFSE prevented HG-induced NOX2 and 4 overexpression and AMPK dephosphorylation in MMCs. PFSE also attenuated ECM, Col IV and fibronectin, protein accumulation in MMCs. These findings suggest that PFSE may serve as a new therapeutic agent of DN.

ACKNOWLEDGMENTS

This research was supported by the Ministry of SMEs and Startups (MSS) and Korea Institute for Advancement of Technology (KIAT) through the Research and Development for Regional Industry (R0004380).

REFERENCES

Banskota S, Regmi SC, Kim JA (2015). "NOX1 to NOX2 switch deactivates AMPK and induces invasive phenotype in colon cancer cells through

overexpression of mmp-7." *Mol. Cancer*. 14: 123.

Calcutt NA, Cooper ME, Kern TS, Schmidt AM (2009). "Therapies for hyperglycaemia-induced diabetic complications: from animal models to clinical trials." *Nat. Rev. Drug Discov.* 8(5): 417-429

Carling D (2017). "AMPK signalling in health and disease." *Curr. Opin. Cell Biol.* 45: 31-37.

Declèves AE, zolklipl Z, Satriano J, Wang L, Nakayama T, Rogac M, Le TP, Nortier JL, Farquhar MG, Naviaux RK, Sharma K (2014). "Regulation of lipid accumulation by AMP-activated kinase (corrected) in high fat diet-induced kidney injury." *kidney Int.* 85(3): 611-623.

Dronavalli S, Duka I, Bakris GL (2008). "The pathogenesis of diabetic nephropathy." *Nat. Clin. Pract. Endocrinol. Metab.* 4(8): 444-452

Dugan LL, You YH, Ali SS, Diamond-stanic M, Miyamoto S, Declèves AE, Andreyev A, Quach T, Ly S, Shekhtman G, Nguyen W, Chepetan A, Le TP, Wang L, Xu M, Paik KP, Fogo A, Viollet B, Murphy A, Brosius F, Naviaux RK, Sharma K (2013). "AMPK dysregulation promotes diabetes-related reduction of superoxide and mitochondrial function." *J. Clin. Invest.* 123(11): 4888-4899.

Erkan N, G Ayranci G, Ayranci E (2008). "Antioxidant activities of rosemary (*Rosmarinus officinalis* L.) extract, blackseed (*nigella sativa* L.) essential oil, carnosic acid, rosmarinic acid and sesamol." *Food Chem.* 110(1): 76-82.

Floege J, Johnson RJ, Gordon K, Iida H, Pritzl P, Yoshimura A., Campbell C, Alpers CE, Couser WG (1991). "Increased synthesis of extracellular matrix in mesangial proliferative nephritis." *Kidney Int.* 40(3): 477-488.

Fridovich I (1997). "Superoxide anion radical (O₂⁻), superoxide dismutases, and related matters." *J. Biol. Chem.* 272(30): 18515-18517.

Gill PS, Wilcox CS (2006). "NADPH oxidases in the kidney." *Antioxid. Redox Signal.* 8(9-10): 1597-1607.

Gorin Y, Block K (2013). "NOX4 and diabetic nephropathy: with a friend like this, who needs enemies?" *Free Radic. Biol. Med.* 61: 130-142.

Hardie DG, Ross FA, Hawley SA (2012). "AMP-activated protein kinase: a target for drugs both ancient and modern." *Chem. Biol.* 19(10): 1222-1236.

Hardie DG, Ross FA, Hawley SA (2012). "AMPK: a nutrient and energy sensor that maintains energy homeostasis." *Nat. Rev. Mol. Cell Biol.* 13(4): 251-262.

Hinchy EC, Gruszczzyk AV, Willows R, Navaratnam N, Hall AR, Bates G, Bright TP, Krieg T, Carling D, Murphy MP (2018). "Mitochondria-derived ROS activate AMP-activated protein kinase (AMPK) indirectly." *J. Biol. Chem.* 293(44): 17208-17217

Hye Kim D, Jun Kim S, Jeong SI, Yu KY, Jin Cheon C, Kim JH, Kim SY (2017). *Perilla frutescens* sprout extracts protected against Cytokine-induced cell damage of pancreatic Rinm5f cells via NF-KB pathway. *J. Life Sci.* 27(5): 509-516

Jeong SI, Kim SJ, Kwon TH, Yu KY, Kim SY (2012). "Schizandrin prevents damage of murine mesangial cells via blocking NADPH oxidase-induced ROS signaling in high glucose." *Food Chem. Toxicol.* 50(3-4): 1045-1053.

Jiang WL, Xu Y, Zhang SP, Hou J, Zhu HB (2012). "Effect of rosmarinic acid on experimental diabetic nephropathy." *Basic Clin. Pharmacol. Toxicol.* 110(4): 390-395.

Kim DH, Kim SJ, Yu KY, Jeong SI, Kim SY (2018). "Anti-hyperglycemic effects and signaling mechanism of *Perilla frutescens* sprout extract." *Nutr. Res. Pract.* 12(1): 20-28.

Kim MY, Lim JH, Youn HH, Hong YA, Yang KS, Park HS, Chung S, Koh SH, Shin SJ, Choi BS, Kim HW, Lee JH, Chang YS, Park CW (2013). "Resveratrol prevents renal lipotoxicity and inhibits mesangial cell glucotoxicity in a manner dependent on the AMPK-SIRT1-PGC1 α axis in *db/db* mice." *Diabetologia.* 56(1): 204-217.

Kim Y, Park CW (2016). "Adenosine monophosphate-activated protein kinase in diabetic nephropathy." *Kidney Res. Clin. Pract.* 35(2): 69-77.

Kumar S (2016). "Obesity and diabetic kidney disease: Role of oxidant stress and redox balance." *Antioxid. Redox Signal.* 25(4): 208-216.

Kume S, Thomas MC, Koya D (2012). "Nutrient sensing, autophagy, and diabetic nephropathy." *Diabetes* 61(1): 23-29.

Lee, MJ, Feliers D, Mariappan MM, Sataranatarajan K, Mahimainathan L, Musi N, Foretz M, Viollet B, Weinberg JM, Choudhury GG, Kasinath BS (2007). "A role for AMP-activated protein kinase in diabetes-induced renal hypertrophy." *Am. J. Physiol. Renal Physiol.* 292(2): F617-F627.

Manickam N, Patel K, Griendling MK, Gorin Y, Barnes JL (2014). "RhoA/Rho kinase mediates TGF- β 1-induced kidney myofibroblast activation

- through Poldip2/Nox4-derived reactive oxygen species." *Am. J. Physiol. Renal Physiol.* 307(2): F159-171.
- Mason RM, Wahab NA (2003). "Extracellular matrix metabolism in diabetic nephropathy." *J. Am. Soc. Nephrol.* 14(5): 1358-1373.
- Nauseef WM (2004). "Assembly of the phagocyte nadph oxidase." *Histochem. Cell Biol.* 122(4): 277-291.
- Petersen M, Simmonds MSJ (2003). "Rosmarinic acid." *Phytochem.* 62(2): 121-125.
- Pompella A, Visvikis A, Paolicchi A, Tata VD, Casini AF (2003). "The changing faces of glutathione, a cellular protagonist." *Biochem. Pharmacol.* 66(8): 1499-1503.
- Ritz E, Rychlík I, Locatelli F, Halimi S (1999). "End-stage renal failure in type 2 diabetes: A medical catastrophe of worldwide dimensions." *Am. J. Kidney Dis.* 34(5): 795-808.
- Sharma K (2014). "Obesity, oxidative stress, and fibrosis in chronic kidney disease." *Kidney Int. Suppl.* 4(1): 113-117.
- Song P, Zou MH (2012). "Regulation of NAD(P)H oxidases by AMPK in cardiovascular systems." *Free Radic. Biol. Med.* 52(9): 1607-1619.
- Xia L, Wang H, Goldberg HJ, Munk S, Fantus IG, Whiteside CI (2006). "Mesangial cell NADPH oxidase upregulation in high glucose is protein kinase C dependent and required for collagen IV expression." *Am. J. Physiol. Renal Physiol.* 290(2): F345-F356.
- Zhang L, Pang S, Deng B, Qian L, Chen J, Zou J, Zheng J, Yang L, Zhang C, Chen X, Liu Z, Le Y (2012). "High glucose induces renal mesangial cell proliferation and fibronectin expression through JNK/NF- κ B/NADPH oxidase/ROS pathway, which is inhibited by resveratrol." *Int. J. Biochem. Cell Biol.* 44(4): 629-638.
- Ziyadeh FN (1993). "The extracellular matrix in diabetic nephropathy." *Am. J. Kidney Dis.* 22(5): 736-744.